Supplementary information

METHODOLOGY

Sedimentology and Geochemistry

Color was analyzed in the L*a*b* color space along a band of approximately 1 mm wide. L* stands for lightness and ranges from 0 (black) to 100 (white). Both a*- and b*-values range from negative (green and blue, respectively) to positive (red and yellow, respectively) (Nederbragt and Thurow, 2004).

Along-core MS was measured with a Bartington MSE2 surface sensor. The along-core resolution of this sensor is 3.5 mm, and the step size during the measurements was 2.5 mm, causing a 1 mm overlap between successive measurements.

For each lake, one master core, which contains EDs that are not or to a limited extent erosional, was selected for more detailed analysis: VILLSC01 (Lake Villarrica) and CAGC02bis (Lake Calafquén).

Sedimentary laminae and layers were imaged with a JEOL 6400 SEM with accelerating voltage of 12 kV.

Grain-size measurements were performed with a Malvern Mastersizer 2000 at a sampling interval of 5 mm, with a measuring time of 15 s on fresh sediment after 60 s of 10% sonification. This was the strongest sonification that could be used without changing the grain-size mode. A longer and/or intenser sonification resulted in a shift of the mode towards lower values, indicating that diatom frustules started to shatter.

For core CAGC02bis, organic-matter (OM) content was determined at 10 mm resolution by loss in ignition (LOI) at 550°C (4 hours) after drying during 24 hours at 105°C.

On selected samples of CAGC02bis, bulk mineralogy was achieved by X-Ray diffraction (XRD) with a Bruker D8-Advance diffractometer with CuKα radiations.

On a selection of tephra layers, glass major element geochemistry was determined on polished grain mounts by electron microprobe analysis (JEOL JXA-8600 Superprobe) at the Research Laboratory for Archaeology and the History of Art, University of Oxford. Calibration was performed using natural mineral standards and accuracy was monitored using natural glass standards. Analyses were performed using 15 kV accelerating voltage, 6 nA beam current and 10 μm beam width. In addition to glass chemistry, mineral compositions were determined semi-quantitatively by SEM-EDS (JEOL JSM-840A) at the Department of Earth Sciences, University of Oxford.

For both lakes, impregnation, lamination counting and μXRF scanning was performed on the master cores. Impregnation was done at RCMG (Ghent University). A new protocol combining the methods of GFZ Potsdam and of Boës and Fagel (2005) was used. A 28 mm wide and 11-mm-thick U-channel spanning the entire core length was taken. The sediment in the U-channel was cut in 100-mm-long sediment slabs with an overlap of 10 mm. Each sample was shock frozen with liquid nitrogen, followed by freeze-drying for 48 hours and slow (approximately 6 hours) impregnation under low vacuum with a mixture of TRA resin, MEKP (catalyst) and cobalt octoate (accelerator), diluted with acetone. One thin section was made for microscopic analysis from the impregnated sediment, while the remainder of the sediment block was polished.

Thin sections and sediment blocks were used for lamination counting, microfacies analysis and μXRF scanning. Lamination-thickness measurements were performed both on the thin sections and on the sediment blocks. The counting and measuring was carried out at the Department of Forest and Water Management (Ghent University), with a RINNTECH LINTAB measuring table, in combination with the TSAPWin software, designed for measuring tree-ring thickness. Micron-scale elemental studies on the sediment blocks were performed by acquiring μXRF spectra with an EDAX EAGLE-III μ-probe (XMI-Group, Ghent University), equipped with a Rh X-ray tube, using a glass polycapillary for X-ray focusing. Source voltage and current were 40 kV and 140 μA respectively, and the measuring time was 11 s/pixel (live time). A small 2D map consisting of five 100 μm spaced scan lines were measured and averaged out. One scan line consisted of successive 100 μm spaced pixels using a μ-beam with about the same radius. Elemental counts represent relative variations in concentration, but are not directly convertible to

absolute elemental concentrations. In order to eliminate density effects in a first order approximation, ratios between two elemental counts were used (Weltje and Tjallingii, 2008).

Chronology

Radionuclide ages were calculated using excess activity of ^{210}Pb ($^{210}Pb_{xs}$), which is incorporated rapidly into the sediment from atmospheric fall-out and water column scavenging. Excess ^{210}Pb was calculated by subtracting the activity supported by its parent isotope, ^{226}Ra, from the total ^{210}Pb activity in the sediment. Errors in $^{210}Pb_{xs}$ were calculated by propagation of errors in the corresponding pair (^{210}Pb and ^{226}Ra). The sedimentation rate was calculated from $^{210}Pb_{xs}$ profiles using the constant initial concentration model (CIC) model (Robbins and Eglington, 1975):

$$t = \frac{1}{\lambda}\ln\left(\frac{A_0}{A}\right)$$

where t is the age (in years) of the considered layer, A_0 and A are the activities of excess ^{210}Pb at surface and depth z, and λ is the decay constant of ^{210}Pb (0.0311 an^{-1}).

To corroborate the ^{210}Pb data, we used also ^{137}Cs, an artificial radionuclide of well-known pulse inputs (maximum nuclear weapon test fall-out in 1965 in the Southern Hemisphere (Arnaud et al., 2006)). ^{210}Pb, ^{226}Ra and ^{137}Cs measurements were performed using a low-background, high-efficiency, well-shaped γ-detector (CANBERRA) (Schmidt et al, 2009). Calibration of the γ-detector was achieved using certified reference materials (IAEA-RGU-1; SOIL-6). Activities are expressed in $mBq.g^{-1}$ and errors are based on 1 standard-deviation counting statistics. For the construction of the radionuclide dated age-depth model, all EDs were removed following the procedure described in von Gunten et al. (2009).

Supplementary Figures

Suppl. Figure 1: A: Rainfall data at the town of Villarrica since 1961, black line: total winter rainfall (May to August), grey line: total yearly rainfall, red dashed lines: El-Niño years; B: Average rainfall per month since 1961; C: comparison of average rainfall in all El-Niño years (A; red line) and "normal" years (black line) shows that El-Niño years are slightly drier (data from Dirección General de Aguas, Chile, unpublished data).

Suppl. Figure 2: Reflection-seismic profiles (sparker and pinger), seismic network and projected coring locations in Lake Villarrica. Interpretation of mass-wasting deposits (MWD) and fluidization structures after Moernaut et al. (2009).

Suppl. Figure 3: Reflection-seismic profiles (sparker and pinger), seismic network and projected coring locations in Lake Calafquén.

Suppl. Figure 4: left: Zoom of the picture in Fig. 4, with EDs indicated; middle: optical microscope images of background sediment and the four types of EDs; right: SEM images of the background sediment and the four types of EDs. EDs are color-coded in the same way as in Fig. 4.

Suppl. Figure 5: Varve age-depth model for VILLSC01 in Lake Villarrica. Grey bar: lacustrine turbidites (LT) in this core; grey dashed line: LTs in other cores; stars: historical earthquakes.

Suppl. Figure 6: Varve age-depth model for CAGC02bis in Lake Calafquén. Grey bar: lacustrine turbidites (LT) in this core; grey dashed line: LTs in other cores; stars: historical earthquakes.

Supplementary Tables

Suppl. Table 1: locations, water depth, length and sampling year of sediment cores discussed in this study.

Suppl. Table 2: historically reported eruptions of Villarrica Volcano including reported VEI and lahars (bold), and the volcanic EDs (light grey) attributed to Villarrica Volcano with varve year and inferred calendar year. Historical earthquakes (EQ) and their corresponding lacustrine turbidites (LT; dark grey) are used as tie-points and added for reference.

Suppl. Table 3: Averaged electron microprobe analyses on glass shards of selected tephra-fall deposits, normalized to 100%. Number of analyzed shards (n°) and if applicable, standard devation (SD) is added.

REFERENCES CITED

Arnaud, F., Magand, O., Chapron, E., Bertrand, S., Boes, X., Charlet, F., and Melieres, M., 2006, Radionuclide dating ((210) Pb,(137) Cs,(241) Am) of recent lake sediments in a highly active geodynamic setting (Lakes Puyehue and Icalma-Chilean Lake District): The Science of the Total Environment, v. 366, p. 837–850, doi:10.1016/j.scitotenv.2005.08.013.

Boës, X., and Fagel, N., 2005, Impregnation method for detecting annual laminae in sediment cores: An overview: Sedimentary Geology, v. 179, p. 185–194, doi:10.1016/j.sedgeo.2005.05.001.

Moernaut, J., De Batist, M., Heirman, K., Van Daele, M., Pino, M., Brümmer, R., and Urrutia, R., 2009, Fluidization of burried mass-wasting deposits in lake sediments and its relevance for paleoseismology: Results from a reflection seismic study of lakes Villarrica and Calafquén (South-Central Chile): Sedimentary Geology, v. 213, p. 121–135, doi:10.1016/j.sedgeo.2008.12.002.

Nederbragt, A.J., and Thurow, J.W., 2004, Digital sediment colour analysis as a method to obtain high resolution climate proxy records, *in* P. Francus (Editor), Image analysis, sediments and paleoenvironments: Kluwer Academic Publishers, Dordrecht, The Netherlands, p. 105-124.

Robbins, J.A., and Eglington, D.N., 1975, Determination of recent sedimentation rates in Lake Michigan using Pb-210 and Cs-137: Geochimica et Cosmochimica Acta, v. 39, p. 285–304, doi:10.1016/0016-7037(75)90198-2.

Schmidt, S., Howa, H., Mouret, A., Lombard, F., Anschutz, P., and Labeyrie, L., 2009, Particle fluxes and recent sediment accumulation on the Aquitanian margin of Bay of Biscay: Continental Shelf Research, v. 29, p. 1044–1052, doi:10.1016/j.csr.2008.11.018.

von Gunten, L., Grosjean, M., Beer, J., Grob, P., Morales, A., and Urrutia, R., 2009, Age modeling of young non-varved lake sediments: methods and limits. Examples from two lakes in Central Chile: Journal of Paleolimnology, v. 42, p. 401–412, doi:10.1007/s10933-008-9284-5.

Weltje, G.J., and Tjallingii, R., 2008, Calibration of XRF core scanners for quantitative geochemical logging of sediment cores: Theory and application: Earth and Planetary Science Letters, v. 274, p. 423–438, doi:10.1016/j.epsl.2008.07.054.

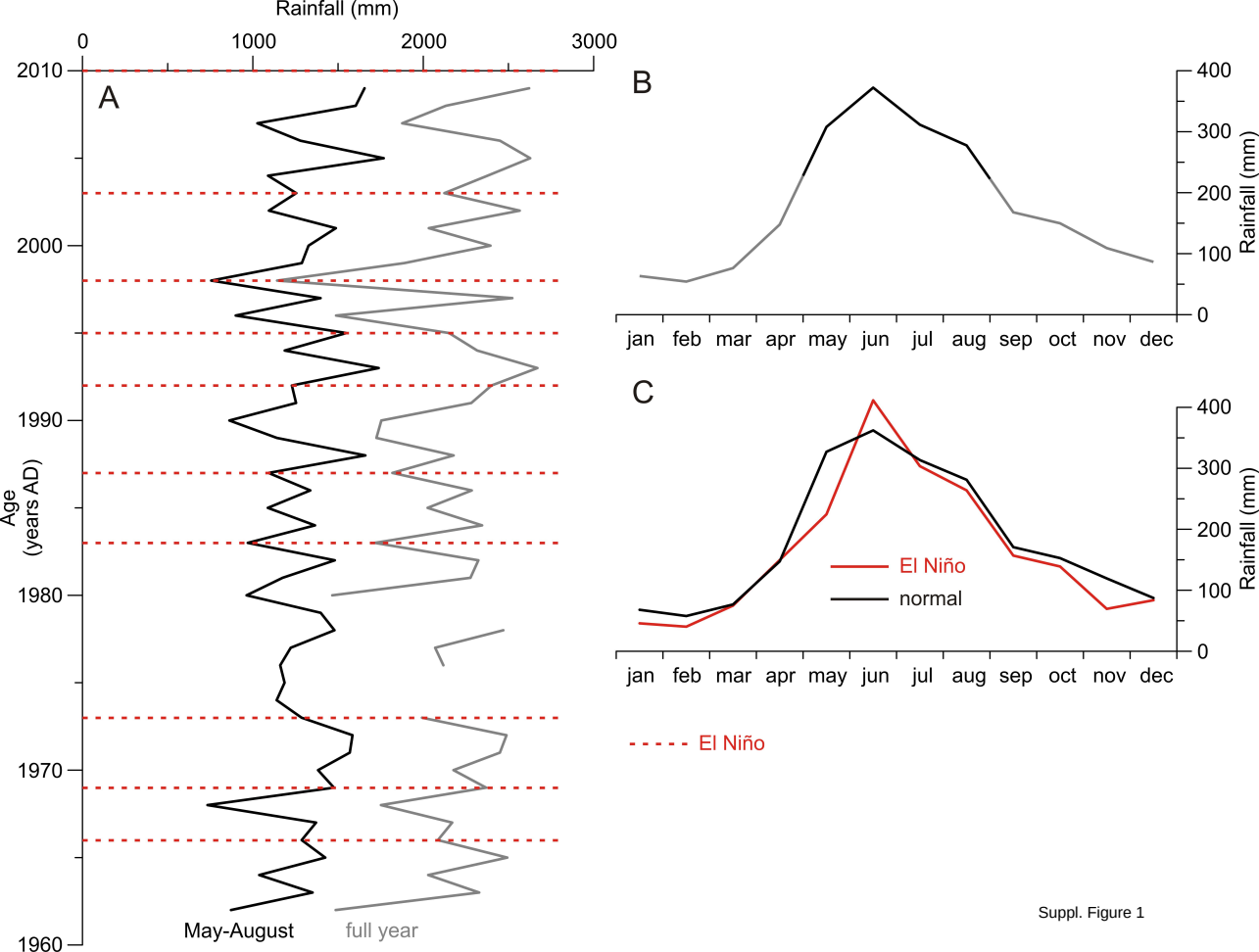

Suppl. Figure 1

Suppl. Figure 2

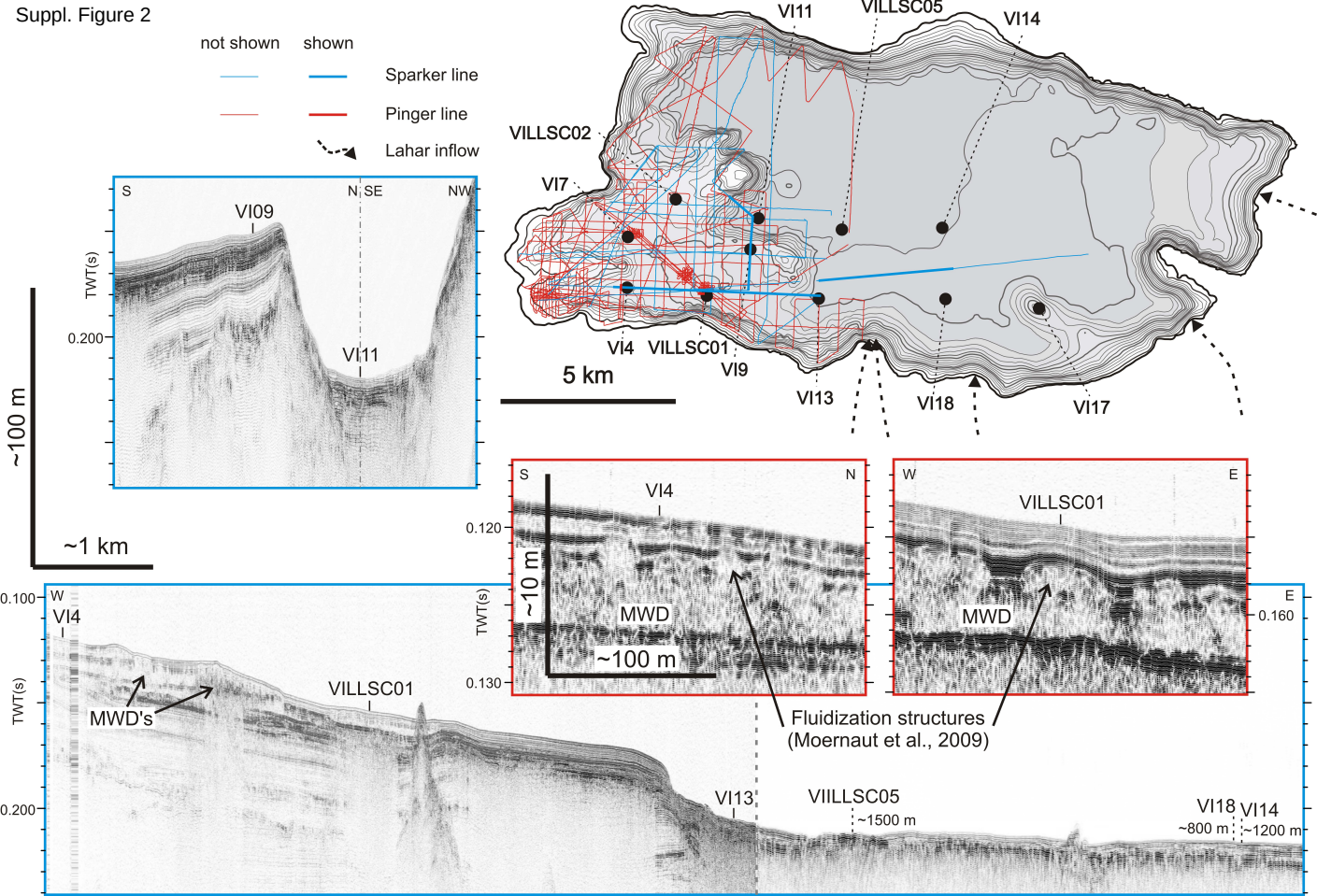

Suppl. Figure 3

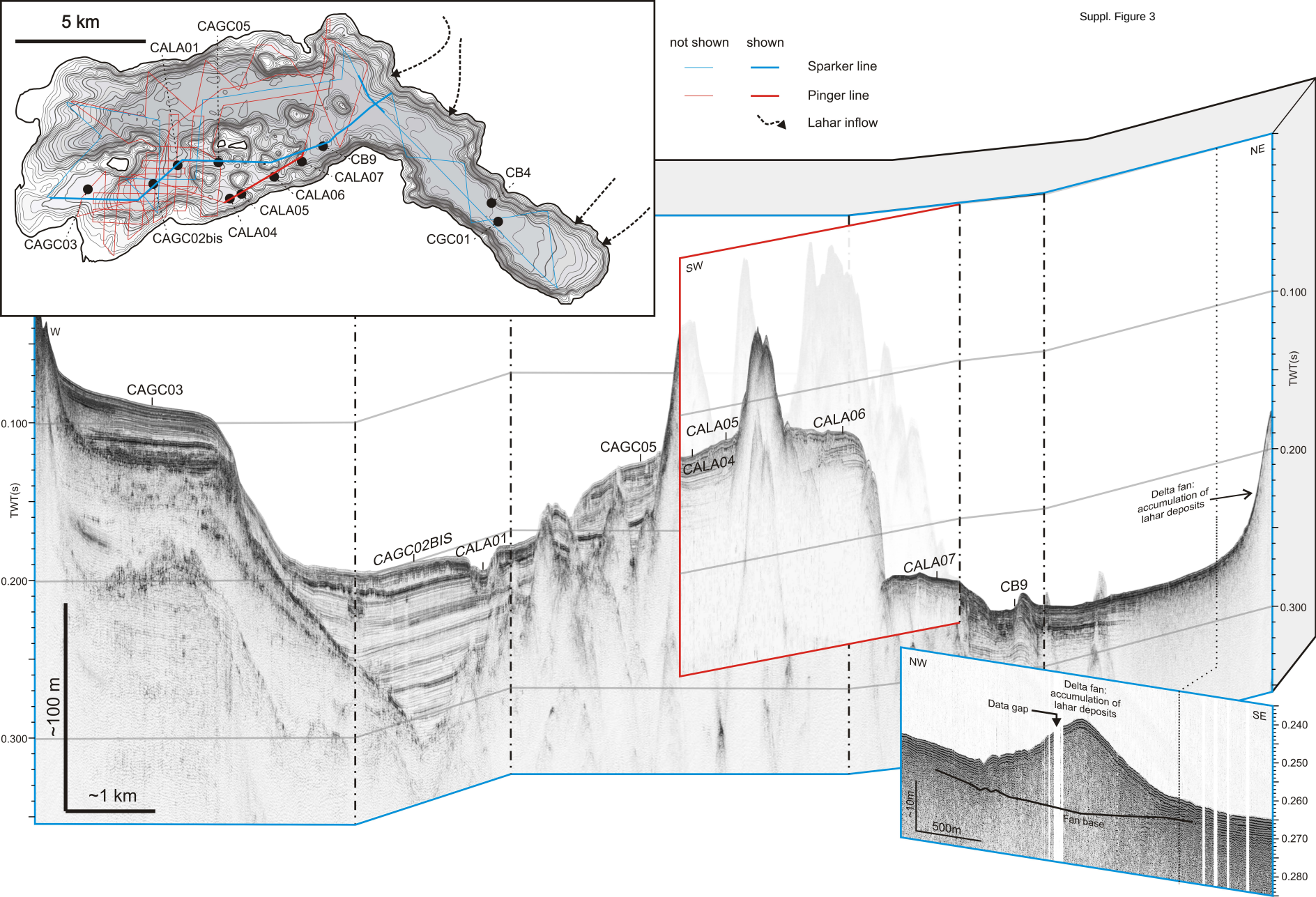

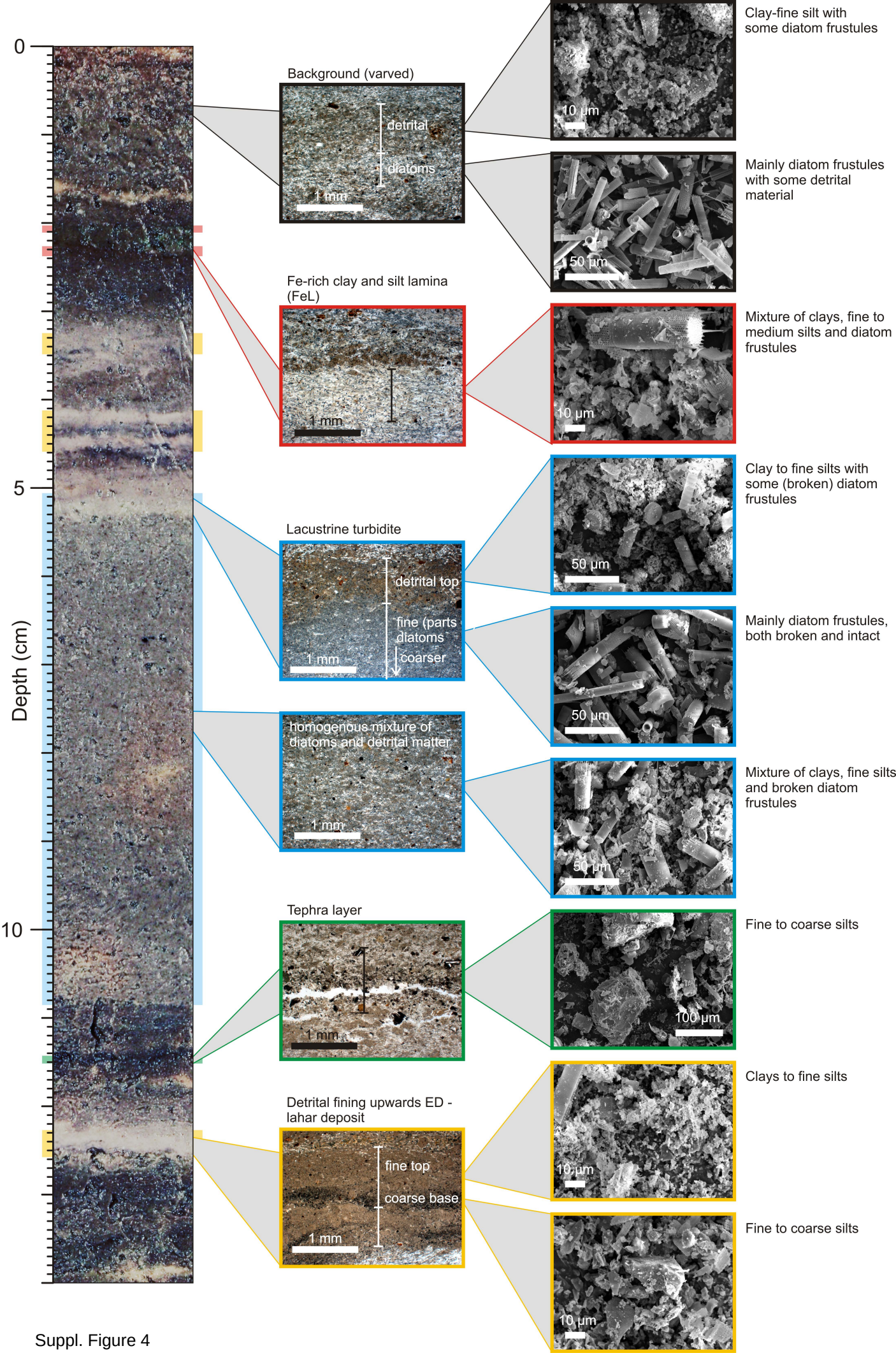

Suppl. Figure 4

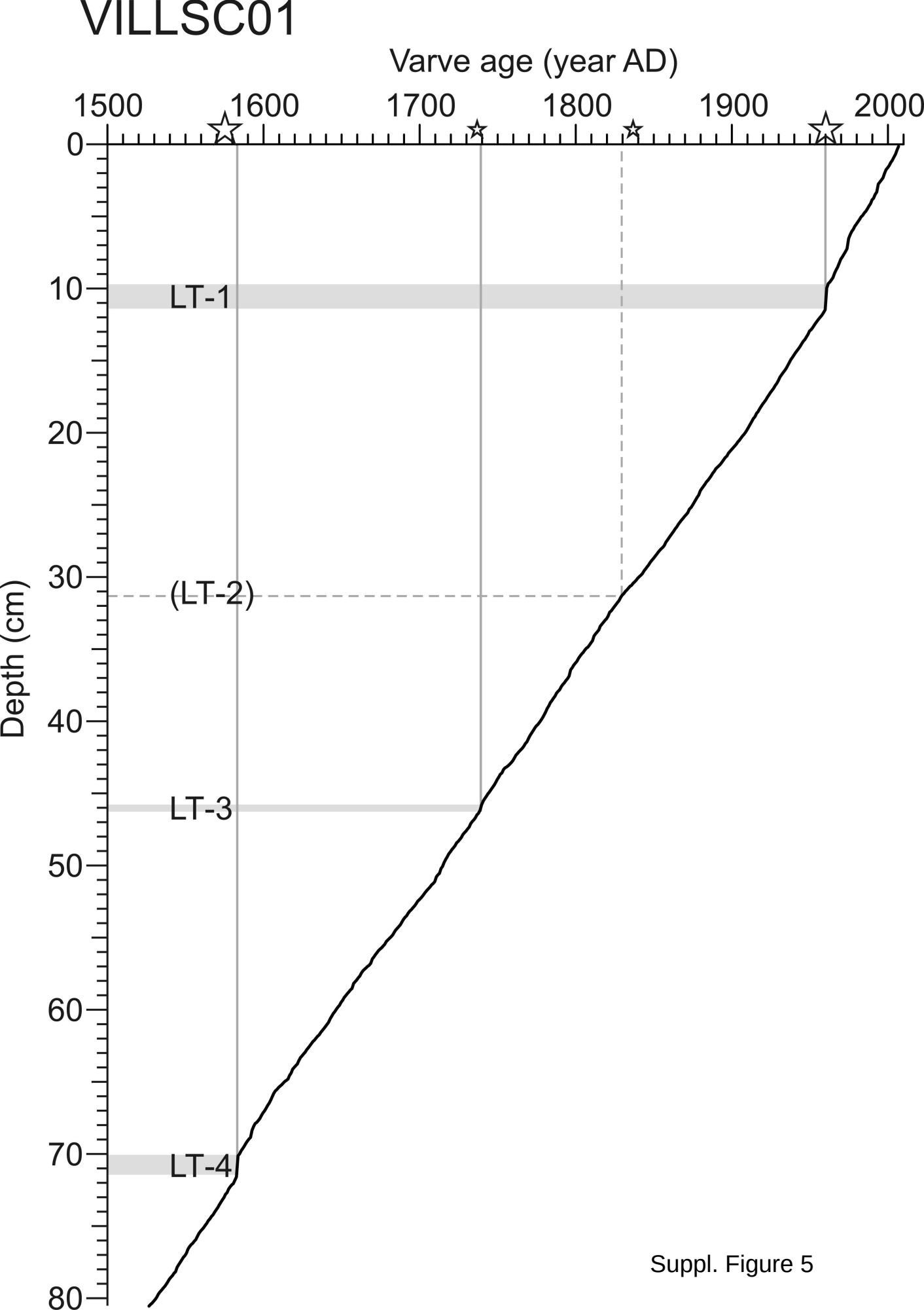

Suppl. Figure 5

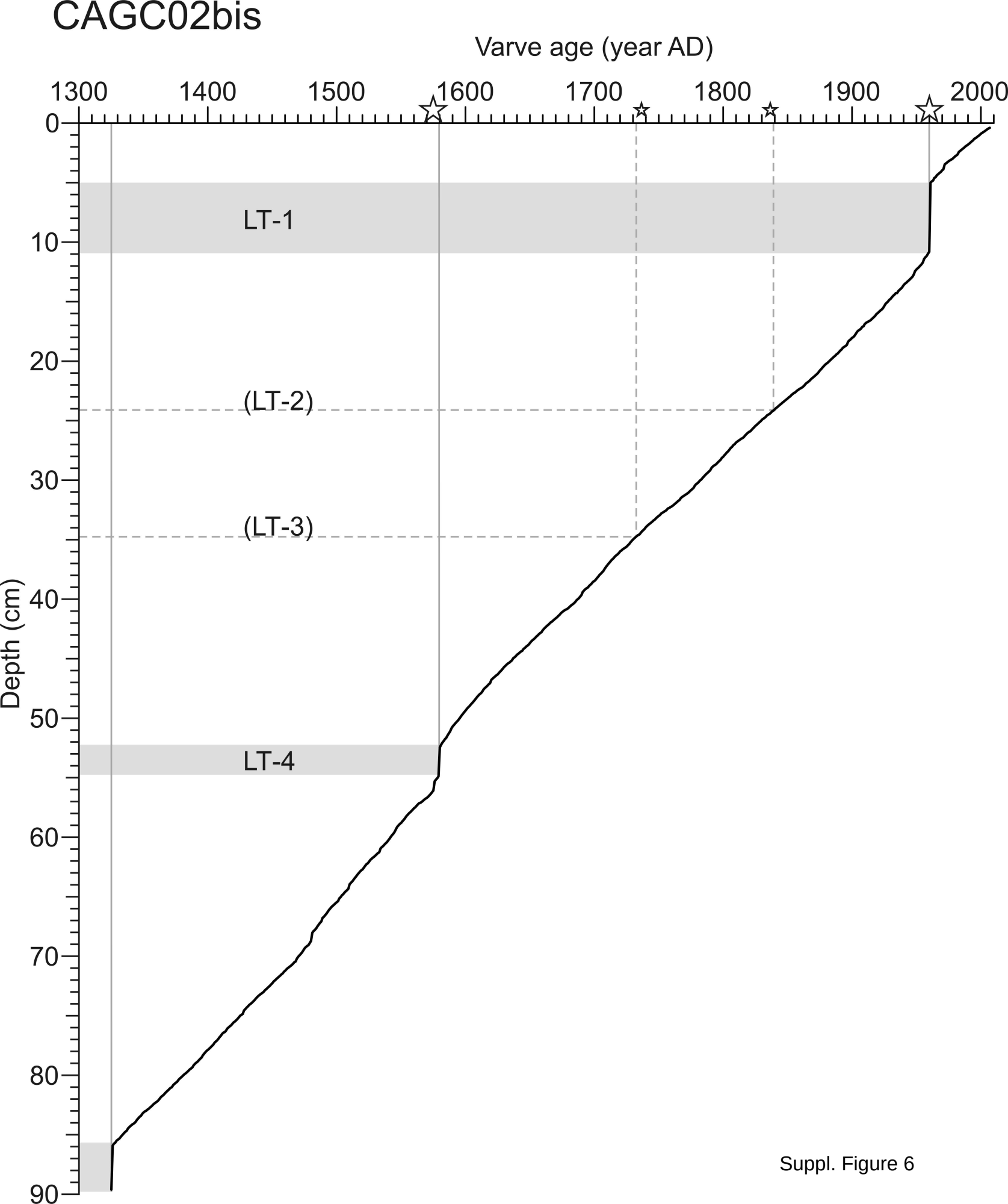

Suppl. Figure 6

Suppl. Table 1

Lake	Core name	Lat (°N)	Long (°E)	Depth (m)	Length (cm)	Sampling year
Villarrica	VILLSC01	-39.28111	-72.14298	112	81	2009
Villarrica	VILLSC02	-39.25664	-72.17123	81	86	2009
Villarrica	VILLSC05	-39.26319	-72.11601	158	49	2009
Villarrica	VI4	-39.28075	-72.1871	85	81	2011
Villarrica	VI7	-39.27097	-72.18065	98	110	2011
Villarrica	VI9	-39.26934	-72.14557	109	106	2011
Villarrica	VI11	-39.26147	-72.14358	160	130	2011
Villarrica	VI13	-39.28201	-72.12283	148	55	2011
Villarrica	VI14	-39.26218	-72.08209	160	59	2011
Villarrica	VI17	-39.28264	-72.04797	90	62	2011
Villarrica	VI18	-39.28082	-72.0803	154	21	2011
Calafquén	CAGC02bis	-39.54586	-72.21898	142	90	2008
Calafquén	CAGC03	-39.54917	-72.25014	63	51	2008
Calafquén	CAGC05	-39.53685	-72.18983	112	76	2008
Calafquén	CB4	-39.5482	-72.06489	173	54	2009
Calafquén	CB9	-39.53046	-72.14298	170	45	2009
Calafquén	CGC01	-39.55566	-72.06033	177	25	2009
Calafquén	CALA01	-39.5397	-72.2099	160	123	2011
Calafquén	CALA04	-39.55054	-72.18385	93	120	2011
Calafquén	CALA05	-39.54848	-72.17941	88	119	2011
Calafquén	CALA06	-39.54146	-72.16435	94	123	2011
Calafquén	CALA07	-39.53595	-72.15231	172	96	2011

Year		Calafquén				Villarrica			
	Rep. VEI	VY	FeL	TEF	LAH	VY	FeL	TEF	LAH
2009	1								
2008	1								
2004	1								
2003	1								
1998	1								
1996	1								
1995	1								
1994	1								
1992	1								
1991	2					1993			X
1984	2	1984	X						
1983	1								
1980	2	1982	X						
1977	1								
1971	**2**	1971			X	1974			X
1964	**2**	1965			X	1965			X
1963	**3**	1963			X	1964			X
1961	1								
1960	1								
1960	EQ	1960		LT-1		1960		LT-1	
1958	1								
1956	1								
1948	**3**	1948			X	1949			X
1948	2?								
1947	1								
1938	2	1938			X				
1935	1								
1933	2					1935	X		
1929	1								
1927	2	1929	X						
1922	2	1924	X						
1921	2?								
1920	**2**					1927			X
1915	1	1918	X						
1909	**2**	1910	X			1918			X
1908	**2**					1916			X
1907	2								
1906	2	1906	X						
1904	**2**	1904	X			1910			X
1902						1908	X		
1897	2					1902			X
1893	2	1894			X	1897			X
1890						1891	X		
1883	2	1887	X						
1880	2					1880			X
1879	2					1878			X
1877	2					1876	X		
1875	2								
1874	2					1872	X		
1871		1877	X						
1869	2	1875	X			1867	X		
1864	2								
1859	2								
1853	2	1860	X			1848		X	
1852						1846			X
1850						1843	X		
1841		1846	X						
1837	2	1841	X						
1837	EQ	1839		LT-2		1830		LT-2	
1836		1839	X						
1832	2	1834	X			1821			X
1826		1829	X			1815	X		
1822	2	1825			X	1811			X
1815	1					1807	X		
1806	2	1807	X			1796			X
1798		1799	X						
1790	1								
1787	2	1790		X		1781			X
1780	1					1775	X		
1777	1								
1775	**2**	1782			X	1772			X
1771		1777	X						
1767		1773	X						

Year		Calafquén				Villarrica			
	Rep. VEI	VY	FeL	TEF	LAH	VY	FeL	TEF	LAH
1761		1766	X						
1759	1	1764	X						
1751	1	1750	X			1753			X
1745	1								
1742	2					1742	X		
1737	2	1734		X		1739	X		
1737	EQ	1732		LT-3		1739		LT-3	
1730	2	1725			X	1728			X
1721		1717			X				
1716	1	1712		X		1715			X
1715						1713	X		
1709		1707	X			1707		X	
1708		1706			X				
1705		1703			X				
1688	**1**	1690			X	1691			X
1682		1684		X		1684			X
1675	?	1676	X						
1672		1673	X						
1669						1672			X
1657	1								
1647	1	1648		X		1651			X
1645						1649	X		
1642						1647	X		
1640		1639			X	1645			X
1638		1637	X						
1632						1638			X
1625		1627	X						
1617		1620			X	1625			X
1612		1617			X	1619			X
1610		1614		X					
1604						1612	X		
1600		1606	X						
1594	2	1601	X			1603	X		
1584		1590	X			1592			X
1582		1587	X						
1579						1587	X		
1576						1584	X		
1575	EQ	1579		LT-4		1583		LT-4	
1564						1577			X
1562	2					1575			X
1558	**2**	1576		X		1571		X	
1553		1571	X			1566	X		
1543		1560	X			1557			X
1539						1551			X
1538						1548	X		
1537						1545	X		
1526		1544	X			1533			X
1523		1541	X						
1521		1539	X						
1516		1534	X						
1515		1533			X				
1509		1527	X						
1503		1521	X						
1497		1515	X						
1494		1512	X						
1492		1510			X				
1483		1501			X				
1479		1497	X						
1474		1492	X						
1471		1489			X				
1466		1484	X						
1463		1481			X				
1454		1472	X						
1448		1466	X						
1433		1451	X						
1417		1435	X						
1413		1431	X						
1410		1428			X				
1404		1422		X					
1392		1410	X						
1388		1406	X						
1384		1402	X						

erosion

Suppl. Table 2

Suppl. Table 3

	Villarrica				Calafquén													
	VT-1		VT-2		CT-1		CT-2		CT-3		CT-5		CT-6		CT-7		CT-8		CT-9	
	wt.%	SD	wt.%	SD	wt.%	SD	wt.%	SD	wt.%	SD	wt.%	SD	wt.%	SD	wt.%	SD	wt.%	SD	wt.%	SD
SiO_2	54,09	0,86	70,54	0,83	57,23		56,82	0,28	57,05		56,21	2,46	56,54	0,33	53,70	0,43	59,52	0,28	70,07	0,81
TiO_2	2,16	0,17	0,65	0,08	1,98		1,53	0,28	2,00		1,54	0,22	1,46	0,06	2,23	0,16	1,38	0,05	0,67	0,08
Al_2O_3	14,72	0,68	14,06	0,35	13,44		15,76	0,92	14,86		14,96	0,58	15,62	0,18	14,14	0,79	15,86	0,17	14,38	0,53
FeO	12,21	0,75	3,92	0,18	12,19		10,07	0,27	11,21		11,05	1,19	9,25	0,18	12,72	0,82	8,32	0,23	3,97	0,32
MnO	0,25	0,06	0,11	0,05	0,38		0,21	0,08	0,17		0,25	0,07	0,18	0,04	0,27	0,05	0,21	0,07	0,13	0,06
MgO	3,29	0,57	0,54	0,12	2,96		2,87	0,34	2,53		3,73	1,15	4,11	0,10	3,37	0,48	2,74	0,06	0,60	0,11
CaO	6,92	0,29	1,88	0,26	6,32		6,91	0,24	6,40		7,22	1,41	7,70	0,17	6,73	0,36	5,76	0,15	2,17	0,33
Na_2O	3,89	0,35	5,06	0,43	3,88		4,53	0,08	4,31		3,79	0,42	3,85	0,20	4,16	0,35	4,64	0,16	5,04	0,22
K_2O	1,90	0,24	3,12	0,46	1,30		0,94	0,28	1,19		0,94	0,20	1,04	0,05	2,13	0,27	1,25	0,04	2,84	0,15
P_2O_5	0,57	0,05	0,12	0,02	0,32		0,37	0,15	0,28		0,29	0,10	0,26	0,02	0,55	0,04	0,31	0,02	0,13	0,03
Total	99,09	0,39	99,30	0,71	98,58		99,02	0,78	99,76		99,10	0,61	99,37	0,53	99,29	0,76	99,54	0,50	99,58	0,44
n°		16		18		1		3		1		11		25		7		21		16